PASSIVE REPEATERS FOR INDOOR SIGNAL RECOVERING

Hristo D. Hristov, Rodolfo Feick, Danilo Torres and Walter Grote

Index terms: wireless communications, mobile communications, propagation

Abstract

The radio signal coverage of indoor areas poses a particularly complex problem in buildings with heavily reinforced concrete or metallic walls, which introduce great attenuation. In these particular conditions, active or passive repeater systems can be implemented for recovering the indoor signal to the level of normal reception. In this paper, we have shown theoretically and demonstrated experimentally the potential for an important improvement of indoor signal coverage by use of a low-cost on-wall passive repeater for the 900-MHz cellular band. It consisted of outside and inside 8-dBi-gain antennas, mounted on a very lossy exterior building wall, and connected through a hole by a piece of coaxial cable and a variable phase shifter in series. We evaluated the effect of the phase shifter on the indoor signal distribution both theoretically and empirically. The average signal recovering efficiency in a room of size 2.6m x 4.6m ranges from 15-17dB near the repeater to about 3 dB at a distance 4 m from the repeater.

1. INTRODUCTION

Assuring adequate signal coverage of indoor areas is an important problem for cellular systems in regions where buildings have high attenuation walls. Active repeaters are often used to solve the problem [1], but in addition to their added cost they need a power supply and maintenance. Also, the amplified signal has the potential of creating significant interference in those areas that are already well covered by a direct signal of the same frequency channel.

In this work we have explored the potential for field coverage improvement by means of two-antenna passive repeaters, similar to those employed in the microwave radio relay links years ago for redirection of wave propagation over hilly terrain [2]. The building passive repeater is a device, which basically consists of two antennas, connected by a cable. In addition, we introduced a novel element to the passive repeater scheme, a phase shifter, aimed at optimizing indoor signal distribution.

Our recent simplified theoretical study [3], has shown that for wall attenuation of less than 10-12 dB (infinite in extent brick walls, single mesh reinforced concrete walls, wooden walls, etc.), the signal enhancement due to the passive repeater with medium gain antennas is moderate. Significant benefits can only be expected at limited ranges or by using high gain antennas at the expense of angular coverage. For the case of a high loss wall however, with attenuation bigger than 20-25 dB, a considerable improvement in indoor signal coverage can be easily achieved.

We propose here three different schemes of building through-wall passive repeaters, but only one of them is analyzed theoretically and studied experimentally: the on-wall mounted passive repeater. It comprises two equal planar antennas, inside and outside, connected through a hole by a piece of cable and a variable phase shifter in series. The average recovering efficiency obtained experimentally in a multipath environment (a small furnished room of size 2.6m x 4.6m ranges), ranges from 15-17 dB near the repeater to about 3dB at a distance 4m from it.

Passive repeaters can of course not be expected to substitute in all cases the need for active radio devices that cover larger areas and that will radiate through windows and other low loss sections of the same construction but as will be seen, under certain conditions they provide significant signal improvement, particularly when limited areas (“hot spots”) must be covered.

2. SOME OUTDOOR-INDOOR PASSIVE REPEATERS

The passive repeater has two antennas, outdoor and indoor, linked by a cable through an exterior wall. It is a two-way transmitting device, but for the purpose of analysis we here assume that the outdoor antenna is receiving and the indoor antenna is transmitting.

Fig. 1 illustrates three possible passive repeater schemes. The first one, A_1-C_1-B_1, has a roof-top vertical antenna A_1, an indoor wall-mounted antenna B_1, and a cable C_1. S is a transmitting base-station antenna and M is the point, where the fixed or mobile wireless unit is located. The power received by A_1 is transferred to B_1, which in turn radiates into the building's inner space. This repeater scheme would be appropriate for mobile cellular links. It has the advantage that the outdoor antenna is omni-directional in the horizontal plane and can receive signals from all cellular base stations within its reach. On the other hand, the connection cable in this scheme may be long and thus lossy, which will naturally decrease the repeater efficiency.

In the second repeater scheme, A_2-C_2-B_2, both antennas, the receiving A_2 and transmitting B_2 are set on the building wall, and are connected by a short piece of coaxial cable C_2 [3]. The antennas can be for instance printed patches over ground plates, which in addition to the lossy wall will ensure very high electromagnetic isolation between them. The scheme is intended for repeating signals from only one or several base stations located in the unidirectional visibility of the antenna A_2. The advantage of this scheme is its compactness and big transfer efficiency, owing to minimal cable losses.

The third repeater scheme, A_3-C_3-B_3, differs from the first one only in the indoor antenna configuration. It is not a single antenna but an array of N distributed antennas $B_3^{(1)}$, $B_3^{(2)}$,..., $B_3^{(N)}$ connected in parallel to a long indoor coaxial cable C_3. The distributed antennas can produce better signal delivery in large indoor areas.

3. TWO-RAY THEORY OF ON-WALL PASSIVE REPEATER

The on-wall passive repeater (second scheme in Fig. 1) can be selectively placed on building walls, small or shielded windows, etc., that for structural or architectonic reasons are built in a way that generates heavy RF absorption.

Fig. 2 illustrates a two-ray model of a cellular link between a base-station S and an indoor mobile telephone M. A plane wave radiated by the antenna at S illuminates the building wall W under the azimuth angle ϕ_i. The elevation incidence angle θ_i is assumed to be zero. The direct ray crosses the wall through the repeater along the path $\overline{\mathrm{SABM}}$. The wall is considered a lossy homogenous plate with a thickness d, relative permittivity ε_r and conductivity σ. The electric and magnetic field vectors and the Poynting vector of the incident wave are labeled by $\vec{E}$, $\vec{H}$ and $\vec{\Pi}$ respectively. If $\vec{E}$ is parallel to the wall and perpendicular to the plane of propagation (as in Fig. 2), the wave polarization is specified as vertical (v). In case of horizontal (h) polarization $\vec{H}$ is parallel to the wall.

The electric field $E_1^{(v,h)}$ at point M, resulting from the wave passing directly through the building wall, can be expressed as a product of the free-space wave E_M (equation A.2) and the complex transmission (refraction) coefficient $T_w^{(v,h)}(\phi_i)$, or

$$E_1^{(v,h)} = E_M T_w^{(v,h)} \tag{1}$$

where $T_w^{(v,h)}(\phi_i) = \left|T_w^{(v,h)}(\phi_i)\right| \exp(j\Psi_{Tw}^{(v,h)}(\phi_i))$. The upper indexes (v,h) refer to vertical or horizontal polarization respectively. We also define the through-wall attenuation as $A_w^{(v,h)}(\phi_i) = 1 \Big/ \left|T_w^{(v,h)}(\phi_i)\right|^2$.

For given d, ε_r and σ, $T_w^{(v,h)}(\phi_i)$ and $A_w^{(v,h)}(\phi_i)$ are easily calculated [4].

The field at each indoor point M is found as a vector sum of the field $E_1^{(v,h)}$ and the field E_2 radiated by antenna B, i.e. in this simplified analysis it is assumed that the secondary waves reflected and transmitted by the other building walls and indoor objects are negligible. Depending on the wave polarization the total field is written as $E^{(v)} = E_1^{(v)} + E_2^{(v)}$, for vertical polarization, and as $E^{(h)} = E_1^{(h)}\cos\phi_i + E_2^{(h)}\cos\phi$, for horizontal polarization.

The analysis that follows is for vertical polarization only, the case of horizontal polarization can be treated in a similar manner. By use of equation (A.8) the field E_2 produced by the on-wall passive repeater at point M can be found, and the total field E can then be expressed in the form

$$E = E_s \cdot \left[\frac{e^{-j\Psi_1}}{\sqrt{A_w(\phi_i)}(s+r')} + \frac{\lambda\sqrt{G_A G_B}}{4\pi\sqrt{A_{rep}}(s+\Delta s)r} F_A(\phi_i)F_B(\phi)e^{-j\Psi_2} \right] \tag{2}$$

where

$E_s = \sqrt{60P_S G_S}e^{-j\beta_0 s}$, with P_s and G_s being respectively the radiation power at the base station antenna and its antenna gain in the direction of the passive repeater;

$\Psi_1 = \beta_0 r' - \Psi(\phi_i)$ and $\Psi_2 = \beta_0\left(\Delta s + \sqrt{\varepsilon_r}d + r\right) - \Psi_\Phi$ are the phase shift angles, corresponding to the direct field E_1 and repeater field E_2; $t = d/\cos\phi_t = d/(\sqrt{1-(\sin^2\phi_i)/\varepsilon_{rc}})$, ($\varepsilon_{rc}$ is the relative permittivity of the cable's dielectric) and $r' = r_0/\cos\phi_i$;

$s + \Delta s$ is the distance between S and A, with $\Delta s = (r_0\tan\phi + r_0\tan\phi_i + d\tan\phi_t)\sin\phi_i$;

$\beta_0 = 2\pi/\lambda$ is the free space phase constant;

$G_A(\phi_i) = G_A F_A^2(\phi_i)$ and $G_B(\phi) = G_B F_B^2(\phi)$ are the directive gains of antennas A and B, with $F_A(\phi_i)$ and $F_B(\phi)$ being the corresponding normalized field radiation patterns;

A_{rep} is the total attenuation factor, which takes into account the antenna, cable and mismatch loss.

We next define the signal recovering efficiency (or gain) as a power ratio g at the receiver point M, which gives the local increase ('amplification') or decrease ('attenuation') of the power density at the receiver point M due to the passive repeater

$$g = \left| \frac{E}{E_1} \right|^2 \tag{3}$$

If the transmitter and receiver points S and M are at positions normal to the repeater, i.e. if $\phi_i = \phi = 0$, then bearing in mind that $s >> r_0$ and $r = r_0$, the power ratio expression can be simplified to

$$g = 1 + 2(Q/r_0)\cos\Psi + Q^2/r_0^2 \tag{4}$$

where

$$\Psi = -\Psi_{rep} - \Psi_w + \Psi_\Phi \tag{5}$$

and

$$Q = \frac{\lambda}{4\pi} \sqrt{\frac{A_w}{A_{rep}}} \sqrt{G_A G_B} \tag{6}$$

For the case of real antenna impedances and low mismatch, the phase-delay angle is equal to $\Psi_{rep} = \Psi_c = \beta_0 \sqrt{\varepsilon_{rc}} d$. As Q is always a positive quantity, it is evident from (4) that the maximum value of the recovering efficiency g is obtained for $\Psi = 0$, or for

$$\Psi_\Phi = \Psi_w + \Psi_{rep} \tag{7}$$

and is given by the following simple expression

$$g_{\max} = \left(1 + \frac{Q}{r_0} \right)^2 \tag{8}$$

For a specific wall, the passive repeater can be tuned for maximum power at the mobile receiver. The repeater delay angle Ψ_{rep} is easily calculated. For a known wall structure and electric parameters the transmission phase angle Ψ_w is also computable. Thus, according to equation (7) the phase-shifter angle can be set to the optimum value of Ψ_Φ. If however, the wall is not specified, the optimum value of Ψ_Φ can be found only by indoor field trials. Also in typical practical cases, multipath propagation will result in a much more complex interference environment making optimum angle prediction very difficult as will be illustrated by our empirical study.

4. NUMERICAL ANALYSIS OF ON-WALL PASSIVE REPEATER

To provide numerical examples for the improvement in signal coverage that can be expected in real situations, we have calculated and contrasted the recovering efficiency for three specific walls of thickness $d = 0.28\,\text{m}$ and infinite extent. It was assumed that these walls can be modeled with acceptable accuracy as homogeneous structures [3]. The incident wave is assumed to be vertically polarized. The walls are described as follows.

(a) brick wall with electric parameters $\varepsilon_r = 4.5$ and $\sigma = 0.02\,\text{S/m}$;

(b) double steel-mesh reinforced concrete wall with $\varepsilon_r = 7$ and $\sigma = 0.1\,\text{S/m}$

(c) extremely lossy (shielded) wall with $\varepsilon_r = 7$ $\sigma = 0.3\,\text{S/m}$.

Reasonable practical values are chosen for the following repeater parameters: $G_A = 20\,\text{dB}$, $G_B = 10\,\text{dB}$ and $A_{rep} = 1.3\,\text{dB}$.

Table 1 lists the computed values of $A_w^{(v)}$ and Ψ_w^v (normal wave incidence) of the above walls for two cellular frequencies: 0.9GHz and 1.8GHz.. The electric parameters ε_r and σ are assumed to be the same for both frequencies.

Table 1 Calculated attenuation $A_w^{(v)}$ and wall phase shift Ψ_w^v in different walls, d =0.28m

Wall Parameters	$f = 0.9$GHz		$f = 1.8$GHz	
	$A_w^{(v)}$,(dB)	Ψ_w^v,(deg)	$A_w^{(v)}$,(dB)	Ψ_w^v,(deg).
Brick, ε_r=4.5, σ =0.02S/m	6	22	5.3	40
Concrete, ε_r=7, σ =0.1S/m	19.5	217	19.3	82
Shielded, ε_r=7, σ =0.3S/m	54.7	170	52	53

Fig. 3 illustrates the calculated recovering efficiency g in the area behind an infinite in extent brick wall vs. the normal distance r_0, for $\phi_i = \phi = 0$ (normal wave incidence) and different values of the extra phase shift Ψ_Φ. The calculations were made for the two cellular frequencies: $f = 0.9$ GHz and $f = 1.8$ GHz. Fig. 4 shows the same relations for a concrete wall. In these figures the recovering efficiency function $g(r_0)$ is drawn for two extreme cases: the best (curves $g_{\max}(r_0)$: solid line for 0.9GHz and dashed line for 1.8GHz) and worst (curves $g_{\min}(r_0)$: dotted line for 0.9GHz and dashed-dotted line for 1.8GHz). It is concluded that for the brick wall the passive repeater is effectively tuned by the phase-shifter, but its potential for signal improvement is moderate and reduces with the distance from the wall. The recovering efficiency can be further increased only by use of more directive antennas (A or/and B).

In the case of a double steel-mesh reinforced concrete wall it is evident that for both frequencies the potential recovering efficiency is much higher for a significant range of distances. The optimum phase shift in this case is $\Psi_\Phi = 0^0$, but as can be seen, close to the wall the repeater signal dominates over the direct ray and the value of the added phase shift becomes less critical. The worst case curves suggest that proper choice of Ψ_Φ is again very important. It must however be stressed that the above figures refer only to the situation at a specific angular position and that

usually the goal is improvement of area coverage. As will be discussed later, our empirical results show that in a practical case, with significant multipath propagation, the average improvement over an area is little affected by the choice of phase shift. This is due to the fact that the phase shift basically changes the position of the regions of constructive and destructive interference, not their size.

The recovering efficiency as a function of the offset distance y (see Fig .2) is illustrated in Fig. 5, for the double steel-mesh reinforced concrete wall (solid line), and for the shielded wall (dashed line). Here the distance r_0 from the receiver point M to the passive repeater is kept constant ($r_0 = 2\,\text{m}$) and $\Psi_\Phi = 0^0$. The frequency is assumed to be $0.9\,\text{GHz}$. For the case of a reinforced concrete wall the recovering efficiency is about 10dB in the offset distance range $y = \pm 0.6\,\text{m}$, while for the shielded wall it has much higher values: 40dB for $y = 0\,\text{m}$ and bigger than 25 dB for in the range $y = \pm 10\,\text{m}$. For the latter case the direct signal is practically zero, and naturally the phase shifter becomes superfluous.

.

5. EXPERIMENTAL STUDY OF TWIN-ANTENNA PASSIVE REPEATER

Complex conditions, such as the effect of multiple arriving wavefronts and reflecting objects, which are difficult to analyze theoretically and which will vary with position inside a room are best treated through an empirical study to collect statistically relevant data. Our procedures described below concentrated on this aspect, providing the results of a real implementation and its comparison with the simplified theoretical model. A passive repeater illuminating a small room is sketched in Fig. 6. Shown are the horizontal room layout and the repeater ray-interference scheme at the receiver point M (direct or transmission ray r', repeater ray r and three reflected rays r_{1r}, r_{2r} and r_{3r}). The room has a width of 2.6m and a length of 4.6m and comprises an exterior brick and mortar wall with a metal door D_1 and partition walls with doors

D_2, D_3 and D_4. The ceiling and the floor are made of reinforced concrete. S_1, S_2 and S_3 are metal stands of size 1.8m (height) x 1.20m x 0.50 m each. The passive repeater device under examination consisted of two equal plane-reflector antennas A and B with vertical polarization, each of size 21cm x 21cm x 5cm, a nominal gain of 8 dB at 900 MHz, VSWR=1.5 and a horizontal-plane beamwidth of 80 degrees. The repeater antennas were mounted on the metal door, at a height of 1.6 m above the floor. In order to increase the through wall attenuation, simulating a high loss wall, the outer side of the wall was loosely covered (shielded) by an anti-mosquito type metal mesh.

The power gain associated with the use of the passive repeater was determined for the case of a continuous wave signal. The procedure involved first measuring the received power in the chosen indoor area, under normal conditions, i.e. when the passive repeater was switched-off. This was done over a wide range of positions in the room according to a square measurement grid of a size equal to one wavelength, or 33.3cm. Both, the transmitter antenna and receiver antenna were held at the repeater's height. The transmitter antenna was placed outdoors at a distance of 7.5m from the shielded wall.

An element of uncertainty in any real situation is the angle of arrival of the outside signal with respect to the boresight of the receiving antenna. Any practical repeater for cellular telephony would be expected to cover a wide azimuth range as the base station position serving a call is not usually known. That is why, the measurements included positioning the transmitter antenna to "see" the passive repeater from several different angles ϕ_i ranging between 0º and 60º, with an increment of 10º. Because the antennas have relatively low directivity, there exists a potential for significant multipath signal propagation, a condition representative of an urban environment. The measured values without the repeater were contrasted with the theoretical free space received power. This provides information on the combined effect of the wall obstructing the direct path, and the multipath interference due to the surrounding building elements and furniture. For each

position inside the room, the corresponding value of received power with the repeater switched-on was subsequently measured. An extra phase-shift, Ψ_ϕ *=0º, 90º, 180º or 270º,* was introduced by means of the phase-shifter in order to test the influence of this parameter. For a plane wave incident on an infinite wall, in an environment devoid of multipath effects the optimum phase shift can be evaluated. However, in the case of a restricted exterior wall in a realistic building room, the presence of multipath propagation implies that the prediction of the influence of the extra phase shift will be virtually impossible and can only be evaluated empirically.

Fig. 7 illustrates the distribution of the power received from the outdoor test transmitter as measured inside the room, when the passive repeater is switched-off. The transmitter antenna is positioned at $\phi_i = 0^o$. The high loss wall with the metal door and repeater is parallel to the yz plane, x=0 (Fig. 6) and the position of the repeater corresponds to the coordinate y=0. Multipath interference is quite pronounced and the power actually increases as one moves away from the wall, indicating that the signal is also entering through the neighboring rooms, with lower loss outside walls. On the average, the measured power level values near the exterior are 26-28 dB lower than predicted by the free space condition.

Fig. 8 presents the power measurements in the same room, if the passive repeater is switched-on and for a normal incidence of the outside wave. Significantly higher power levels are observed with multipath fluctuations that are similar to those when the repeater is switched-off.

Figure 9 shows the theoretical levels calculated by use of the simple model discussed before, considering an infinite wall, with an attenuation of 28dB. The calculations were done for a normal wave incidence. Obviously, the multi-ray fluctuations are not present here, but it is interesting to observe that the mean power levels do not differ very much from those in Fig. 8, especially up to distances of 2-3 m. At very short range where the repeater power is dominant both graphs are quite similar.

For Fig. 8 and Fig. 9 the extra phase shift between repeater antennas was chosen to be 270º, a value that results in good gain and smooth coverage. Measurements performed for other values of the phase shift show similar results. As expected, it was observed that in the region where the repeater power dominates, the phase shift is of little consequence. In contrast, in the region where the repeater output is comparable to the signals entering through the walls, the diagram changes significantly. Interestingly though, it was found that on the average, the total area with relevant signal gain tends to remain unchanged and thus the search for an "optimal phase shift" will be limited to cases where only specific points in a room need signal improvement and where multipath propagation plays no significant role.

The large amount of collected data, and the variations that are to be expected for these type of measurements, requires the use of statistical processing of data in order to be able to draw general conclusions. From the measured power data we calculated the average recovering efficiency at a given distance from the repeater wall: g_{av} (dB)=P(dBm)–P_1 (dBm). Here P and P_1 are, respectively, the average (in dBm) power levels that correspond to the switched-on and switched-off conditions of the passive repeater. The averaging was done over all angles of incidence and for all measurement points in each mesh line parallel to the y-axis (Fig. 6). The average recovering efficiency curves as function of distance from the repeater to the door D_4 are drawn in Fig. 10, for two values of the phase shift Ψ_Φ : 90º–dashed line (best case) and 180º– dashed dotted line (worst case). The continuous line in the same figure illustrates as a reference, the theoretical function $g(r_0)$, for the ideal case of a transmitter and receiver located on the axis of the repeater antenna beams. It was calculated by use of equation (3), for A_w=28dB, $A_{rep} = 1.3\,\text{dB}$, $\Psi_\Phi = 90^o$ and $G_A = G_B$=8 dB. As can be seen, on average, the difference between best and worst case is not big, far less than the extreme conditions depicted in figures 3 and 4. It is evident that the signal average signal recovering efficiency oscillates and decreases

quickly with the distance, ranging from about 15 dB near the repeater, to about 3 dB at the far end of the room.

CONCLUSIONS

We have shown theoretically and demonstrated experimentally the potential for a significant improvement of indoor signal coverage by use of an on-wall-wall passive repeater for the 900-MHz cellular band. To the classical repeating scheme a new element was introduced – a tuning phase shifter – and its influence evaluated. For the idealized case of an infinite homogeneous the two-ray interference scheme predicts that the phase shifter role depends much on the wall character: it can be an important element for low and medium loss walls (brick, single mesh reinforced concrete, wood, etc); for very high loss concrete or metallic walls its role is of little significance. Our empirical work confirmed that for the specific case of a small building room with a high loss exterior wall and a realistic indoor environment, significant signal recovering is achieved, ranging from 15-17 to about 3 dB depending on the position in the room. The effect of the extra phase shift is important when certain specific zones in the room need signal improvement. Multipath propagation tends in practice to make the choice uncritical when larger areas need to be covered, as improvements in a certain region due to the choice of the proper phase shift are offset by deterioration in other areas. The feasibility of predicting optimum values for the phase shift is restricted to cases where a simple propagation environment makes a theoretical analysis practical.

While our analysis stressed the improvement in signal coverage over a complete area (mobile situation), for the case of fixed-terminal communication systems the signal level can be further increased using more directive repeater antennas or antenna arrays that cover only certain angular positions.

ACKNOWLEDGEMENT

The authors acknowledge the support received by the Chilean National Science Agency CONICYT through the Fondecyt project # 1010129/2001.

REFERENCES

1. Repeater Technologies, http://www.repeaters.com

2. G. Z Aizenberg and B. G. Yampolskii, "Passive repeaters for radio relay links", Svyaz Publ., 1973 (in Russian).

3. H. D. Hristov, R. Feick, and W. Grote, "Improving indoor signal coverage by use of through wall passive repeaters", *IEEE Antennas Propag. Soc. Int. AP-S Symp. Digest*, Boston, vol. 2, 2001, pp. 158-161.

4. W. D. Burnside and K. W. Burgener "High frequency scattering by a thin lossless dielectric slab", *IEEE Trans. A P-S*, vol 31, Nº 1, 1983, pp. 104-110.

Appendix

Basic Equations for Passive Signal Repeating

The power P'_M received by the receiver antenna M in the case of direct free space propagation along a path $s+r$ is found by the Friis wireless link equation, or

$$P'_M(\phi,\theta)=\left(\frac{\lambda}{4\pi(s+r)}\right)^2 P_S G_S(\phi,\theta) G_M(\phi,\theta) \qquad \text{(A.1)}$$

where the P_S is the power radiated by the base-station antenna S; $G_S(\phi,\theta)=G_S F_S^2(\phi,\theta)$ and $G_M(\phi,\theta)=G_M F_M^2(\phi,\theta)$ are gain functions expressed by their maximum values G_S and G_M, and normalized field radiation patterns $F_A(\phi,\theta)$ and $F_B(\phi,\theta)$, respectively.

The corresponding electric field E'_M at the point M is given by

$$E'_M(\phi,\theta) = \frac{\sqrt{60 P_S G_S(\phi,\theta)}}{s+r} e^{-j\beta.(s+r)} \tag{A.2}$$

If the signal is not propagating directly from point S to point M, but through a passive two-antenna repeater (Fig. 2), the power at the mobile antenna output can be found as follows.

The power P_A in the receiving repeater antenna A can be also found by use of the Friis equation, applied to the path s only, or

$$P_A(\phi,\theta) = P_s\left(\frac{\lambda}{4\pi s}\right)^2 G_s(\phi,\theta) G_A(\phi,\theta) \tag{A.3}$$

with $G_A(\phi,\theta) = G_A F_A^2(\phi,\theta)$ being the gain pattern of antenna A.

The power at the input of transmitting repeater antenna B is proportional to the power P_A, or

$$P_B(\phi,\theta) = \eta_c P_A(\phi,\theta) \tag{A.4}$$

where the total cable efficiency η_c, calculated by the equation

$$\eta_c = e^{-2\alpha_c l_c}\left(1-\rho_A^2\right)\left(1-\rho_B^2\right) \tag{A.5}$$

η_c is a product between the cable loss efficiency $\eta_l = e^{-2\alpha_c l_c}$ and the match efficiencies $1-\rho_A^2$ and $1-\rho_B^2$. Here ρ_A and ρ_B are the reflection coefficients at the ports of repeater antennas.

After inserting P_A from (A.3) into (A.4) we find

$$P_B(\phi,\theta) = \left(\frac{\lambda}{4\pi s}\right)^2 \eta_c P_S G_s(\phi,\theta) G_A(\phi,\theta) G_B(\phi,\theta) \tag{A.6}$$

The electric field $E''_M(\phi,\theta)$ at the receive point M can expressed in the form

$$E''_M(\phi,\theta) = \frac{\sqrt{60 P_B G_B(\phi,\theta)}}{r} e^{-j\beta.r} \tag{A.7}$$

and after replacing $P_B(\phi,\theta)$ by its expression from (A.6) the equation

for $E''_M(\phi,\theta)$ becomes

$$E''_M(\phi,\theta) = \frac{\lambda}{4\pi sr}\sqrt{60\eta_c P_S G_S(\phi,\theta) G_A(\phi,\theta) G_B(\phi,\theta)}\, e^{-j(\beta . r + \Psi)} \qquad (A.8)$$

where

$\beta = 2\pi / \lambda$ is the free-space phase constant;

$\Psi = \beta(s + \sqrt{\varepsilon_r} l_c)$ is the phase shift produced by the free-space wave traveling along the path s and by the repeater coaxial cable of length l_c and relative dielectric constant ε_r.

The power $P''_M(\phi,\theta)$ in the mobile antenna M, located in the far field of antenna B, is calculated by the equation

$$P''_M(\phi,\theta) = \left|E''_M(\phi,\theta)\right|^2 \frac{\lambda^2}{960\pi^2} G_M(\phi,\theta) \qquad (A.9)$$

Inserting $\left|E''_M(\phi,\theta)\right|$ from (A.8) into (A.9) leads to

$$P''_M(\phi,\theta) = P_S G_S \left(\frac{\lambda}{4\pi}\right)^4 \left(\frac{1}{sr}\right)^2 \eta_c G_A(\phi,\theta) G_B(\phi,\theta) G_M(\phi,\theta) \qquad (A.10)$$

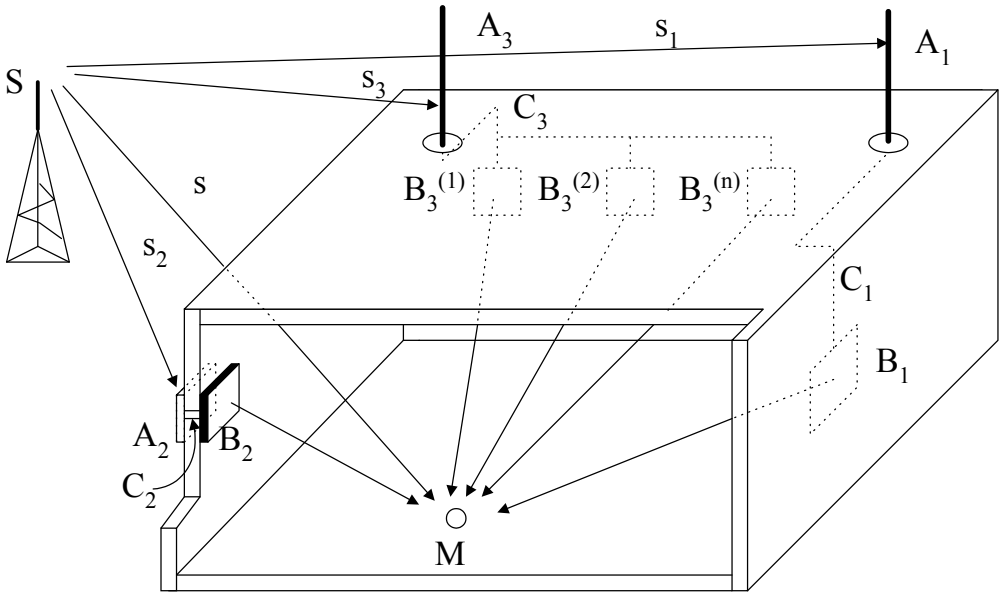

Figure 1. Passive repeater schemes

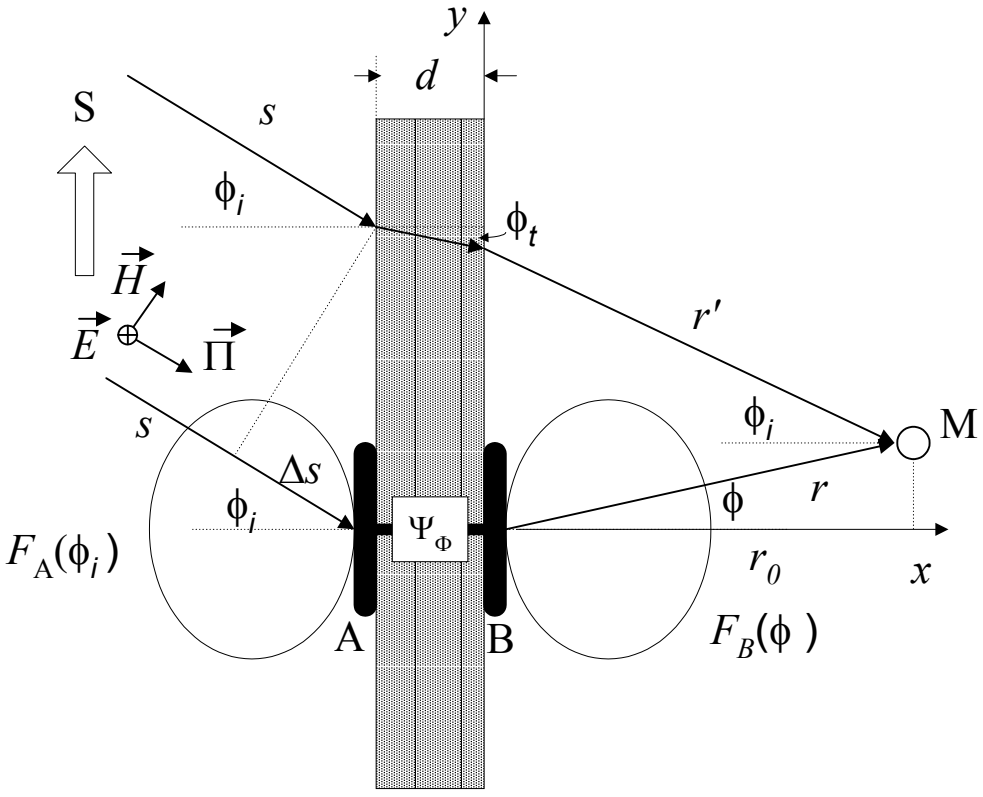

Figure 2. On-wall passive repeater geometry: two-ray scheme

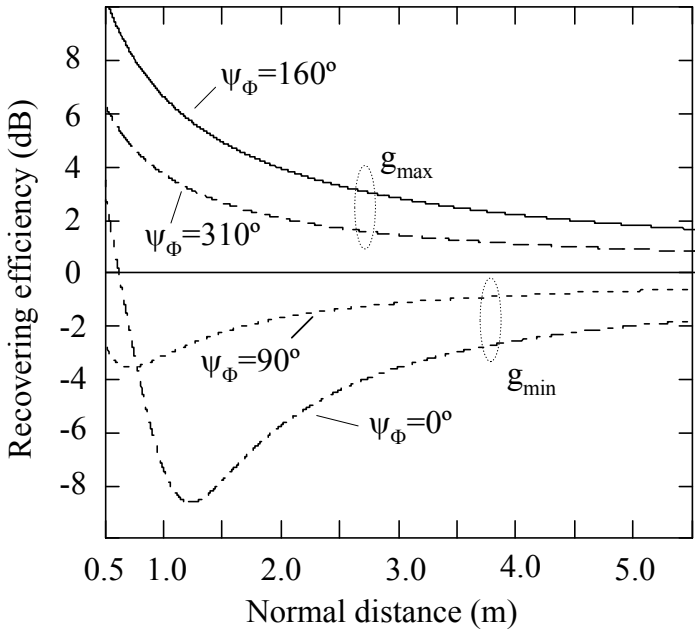

Figure 3. Recovering efficiency vs. distance r_0 for brick wall (f=0.9GHz solid and dotted, f=1.8GHz dashed and dash-dotted)

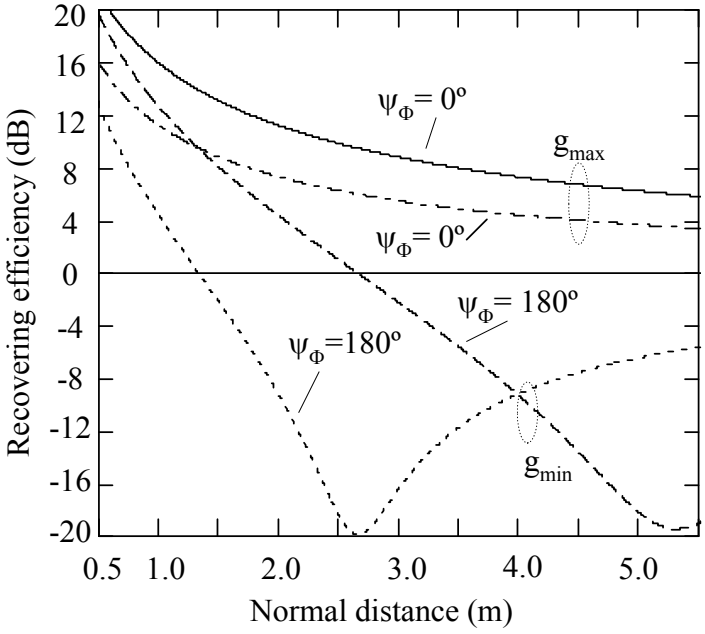

Figure 4. Recovering efficiency vs. distance r_0 for concrete wall (f=0.9GHz solid and dotted, f=1.8GHz dashed and dash-dotted)

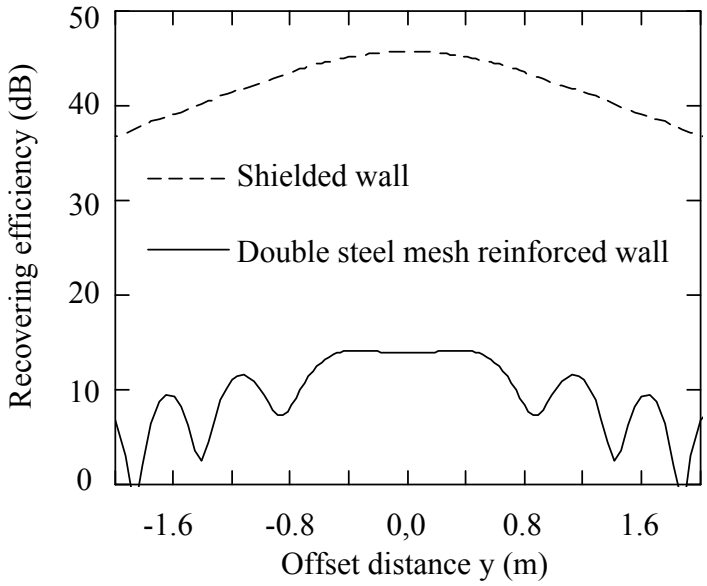

Figure 5. Power gain vs. distance y, concrete wall

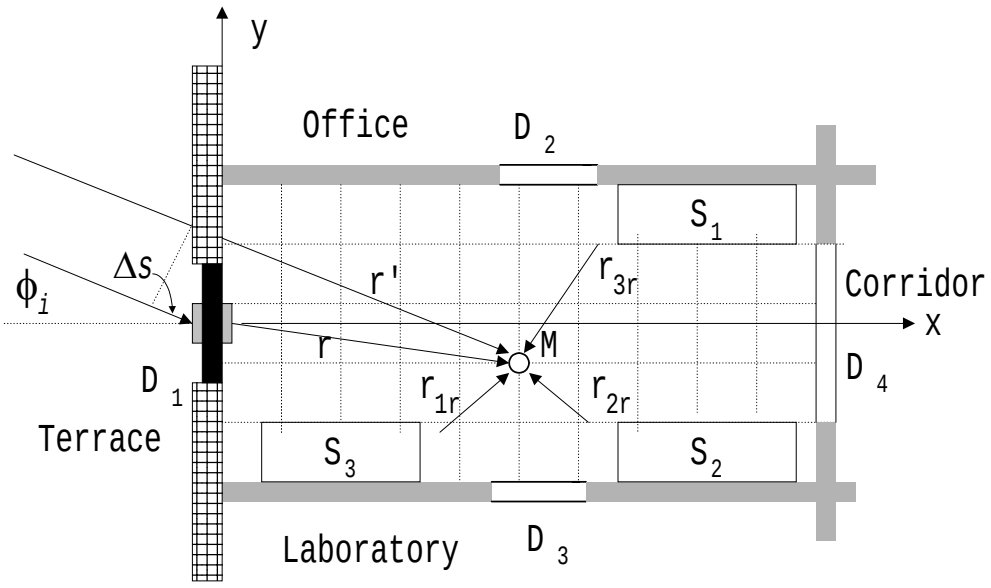

Figure 6. Passive repeater illuminating small room: horizontal-plane layout

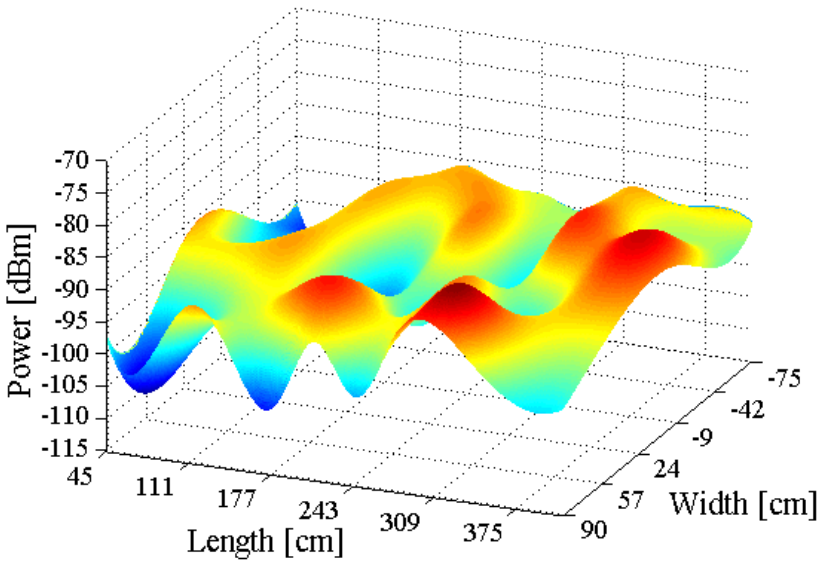

Figure 7. Measured received power: repeater switched-off and angle of incidence ϕ_i =0º

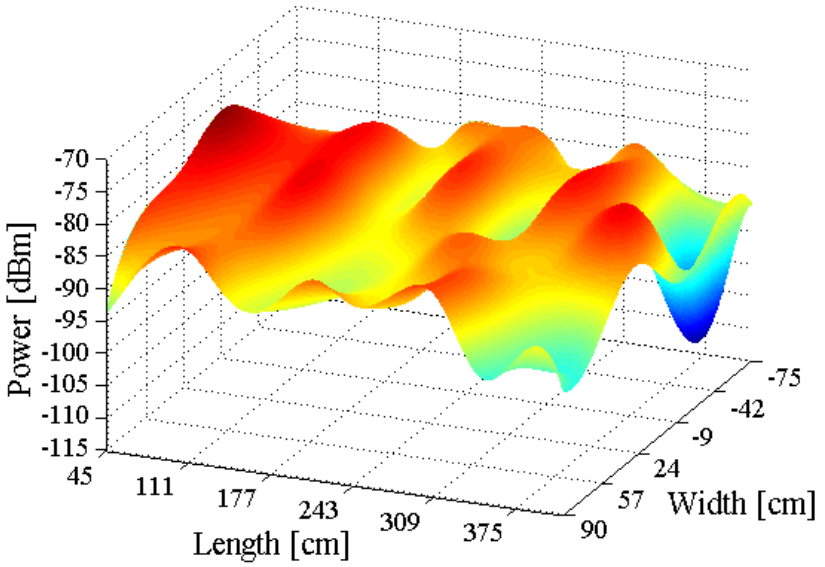

Figure 8. Measured received power: repeater switched-on (ϕ_i =0º and Ψ_ϕ =270º)

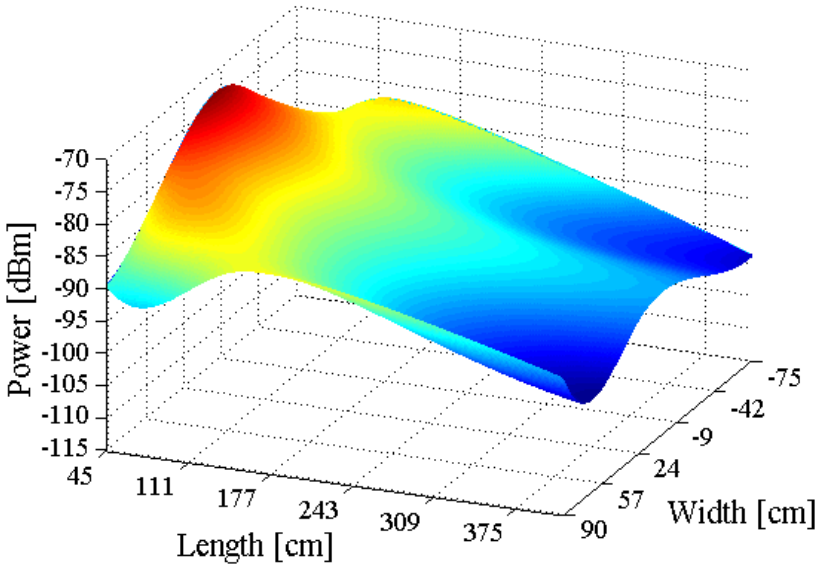

Figure 9. Theoretical received power with passive repeater switched-on (ϕ_i =0º and Ψ_ϕ =270º)

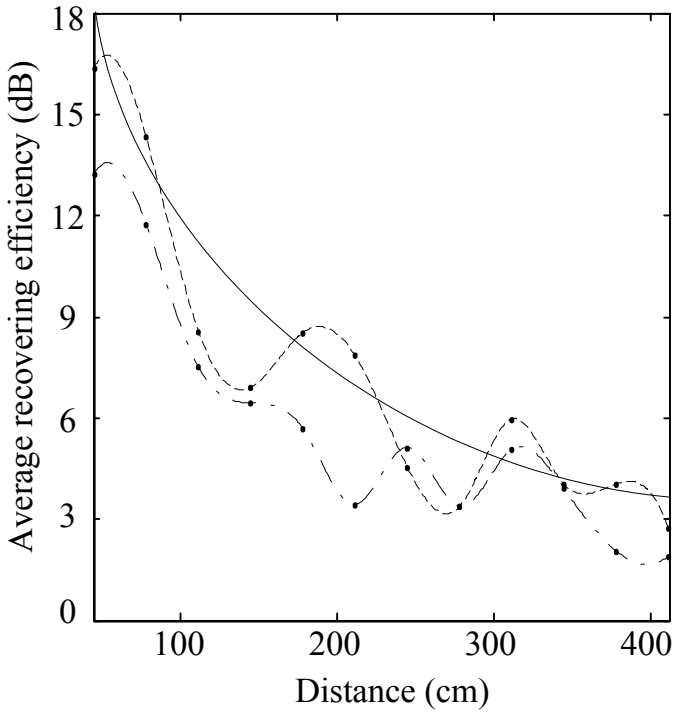

Figure 10. Average recovering efficiency g vs. normal distance r_0 of on-wall passive repeater: experimental curves, for two phase shift values: Ψ_Φ =90º (dashed line) and Ψ_Φ =180º (dash-dotted line), and theoretical curve (solid line) for Ψ_Φ =90º, receiver and transmitter on axis of antenna lobes.